

SU(3) centre vortex geometry at finite temperature

Jackson A. Mickley, Waseem Kamleh and Derek B. Leinweber*

Centre for the Subatomic Structure of Matter, Department of Physics, The University of Adelaide, South Australia 5005, Australia

E-mail: jackson.mickley@adelaide.edu.au, derek.leinweber@adelaide.edu.au

The importance of examining the structure of centre-vortex matter in the ground-state fields of nonabelian gauge-field theory has been demonstrated in the recent centre-vortex based discovery of a second finite-temperature transition in QCD associated with quark deconfinement. This signals the presence of a new phase of ground-state field structure between the well separated chiral and deconfinement transitions. In this short presentation, we re-examine pure SU(3) gauge theory which provides a foundation for the development of techniques for the examination of full QCD. This time, we reconsider visualisations of the centre-vortex structure in light of the quantitative analysis that demonstrates the first order nature of the deconfinement phase transition in the pure-gauge theory. Here we consider a detailed side-by-side comparison of the field structure slightly below and slightly above the critical temperature. The abrupt changes of the field structure in the first order phase transition are easy to observe in the representative visualisations.

The XVIth Quark Confinement and the Hadron Spectrum Conference (QCHSC24)
19-24 August, 2024
Cairns Convention Centre, Cairns, Queensland, Australia

*Speaker

1. Introduction

Through an examination of centre-vortex matter in the ground-state fields of QCD and the dependence of its structure on temperature [1], a second finite-temperature transition associated with quark deconfinement has been discovered [2]. The discovery of a new phase of QCD ground-state field structure between the well separated chiral and deconfinement transitions emphasises the importance of examining centre-vortex structure [3–33] in QCD. For more recent overviews see Refs. [34, 35].

The visualisation and animation of centre-vortex structure is helpful in understanding the nature of vortex matter and vital to the formulation of new measures to quantify its structure. Good examples of this include the novel vortex persistence correlation measure [1], the role of secondary clusters as a signature of deconfinement [1], and the rigorous definition of a vortex branching probability [31].

In this short presentation, we re-examine pure SU(3) gauge theory [1] which provides a foundation for the development of techniques for the examination of full QCD [2]. This time, we reconsider visualisations of the centre-vortex structure in light of the quantitative analysis of Ref. [1] that demonstrates the first order nature of the deconfinement phase transition in the pure-gauge theory.

Here we consider a detailed side-by-side comparison of the vortex-matter field structure slightly below and slightly above the critical temperature. Drawing on the quantitative analysis presented in the figures of Ref. [1], we'll search for signatures of the established properties in the representative illustrations of the field structure. The abrupt step changes of the field structure in the first order phase transition are easy to observe in the visualisations and animations.

We begin with a brief review of centre vortex identification and visualisation techniques in the following section. The detailed examination of the field structure follows in Sec. 3 where interactive 3D visualisations and animations are presented. We close with a few concluding remarks.

2. Centre-vortex visualisation techniques

Physical vortices in the QCD ground-state fields have a finite thickness and so permeate all four spacetime dimensions. In contrast, on the lattice “thin” centre vortices are extracted through a well-known gauge-fixing procedure that seeks to bring each link variable $U_\mu(x)$ as close as possible to an element of \mathbb{Z}_3 . This is known as Maximal Centre Gauge (MCG).

Fixing to MCG is typically performed by finding the gauge transformation $\Omega(x)$ to maximise the functional [9]

$$R = \frac{1}{V N_{\text{dim}} N_c^2} \sum_{x, \mu} \left| \text{Tr } U_\mu^\Omega(x) \right|^2, \quad V = N_s^3 \times N_\tau. \quad (1)$$

The links are subsequently projected onto the centre,

$$U_\mu(x) \longrightarrow Z_\mu(x) = \exp \left(\frac{2\pi i}{3} n_\mu(x) \right) \mathbb{I} \in \mathbb{Z}_3, \quad (2)$$

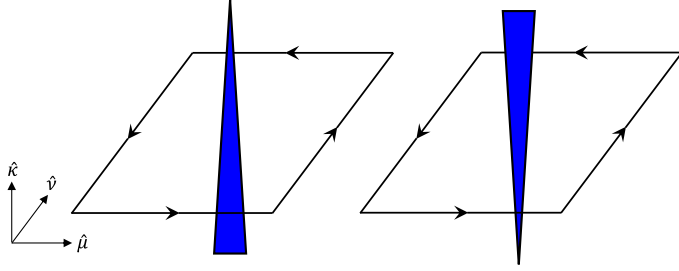


Figure 1: The visualisation convention for centre vortices. An $m = +1$ vortex (**left**) is represented by a jet in the available orthogonal dimension, with the direction given by the right-hand rule. An $m = -1$ vortex (**right**) is rendered by a jet in the opposite direction.

with $n_\mu(x) \in \{-1, 0, 1\}$ identified as the centre phase nearest to $\arg \text{Tr } U_\mu(x)$ for each link. Finally, the locations of vortices are identified by nontrivial plaquettes in the centre-projected field

$$P_{\mu\nu}(x) = \prod_{\square} Z_\mu(x) = \exp\left(\frac{2\pi i}{3} m_{\mu\nu}(x)\right) \mathbb{I} \quad (3)$$

with $m_{\mu\nu}(x)$ having nontrivial values ± 1 . The value of $m_{\mu\nu}(x)$ is referred to as the *centre charge* of the vortex, and we say the plaquette is pierced by a vortex. The centre charge is conserved such that the vortex topology manifests as closed sheets in four dimensions, or as closed lines in three-dimensional slices of the lattice.

With the locations of vortices identified, we draw on the visualisation techniques previously established in Ref. [26]. To construct a 3D visualisation we slice on a given dimension. For example temporal slices have the time coordinate, τ , fixed, whereas spatial slices have one of the spatial coordinates, x , y , or z , fixed. This leaves one direction orthogonal to a non-trivial plaquette that can be used to identify the sign of the centre charge. As vortices exist on the dual lattice, the point-like centre vortex for

$$P_{\mu\nu}(x) = \exp\left(\frac{2\pi i}{3} m_{\mu\nu}(x)\right), \quad (4)$$

is plotted at the centre of the plaquette. As the centre charge can take values of ± 1 we render this information as a jet pointing in the third dimension orthogonal to the μ - ν plane with values of $+1$ (-1) pointing in the positive (negative) direction. As such, the visualisations exclusively show the flow of $m = +1$ centre charge. This convention is demonstrated in Fig. 1. Finally, utilising the SU(3) cluster identification algorithm developed in Ref. [31], the percolating cluster is rendered with blue jets and secondary vortex cluster loops are rendered in contrasting colours to aid in their identification.

The connection between centre vortices and confinement is apparent through space-time Wilson loops of size $R \times T$, which asymptotically give access to the static quark potential $V(r)$

$$\langle W(R, T) \rangle \sim \exp(-V(r) a T), \quad r = Ra, \quad T \text{ large}. \quad (5)$$

The percolation of centre vortices through spacetime at low temperatures provides an area law for the Wilson loop corresponding to a potential $V(r)$ that linearly rises with the separation r . Thus in examining the centre-vortex structure that gives rise to confinement, it will be essential to render spatial slices of the lattice such that vortices piercing space-time plaquettes can be observed.

3. Changes in vortex-matter structure through the deconfinement phase transition

3.1 Temporal Slices

3.1.1 Overview

We begin by studying the more intuitive temporal slices of the finite temperature lattices of Ref. [1] where the temporal coordinate is held fixed and the spatial volume is visualised. The lattices have a fixed isotropic lattice spacing $a = 0.1$ fm and a spatial volume of 32^3 . The ensembles were generated with the Iwasaki renormalisation-group improved action [36].

Here we examine two temperatures very close to the critical temperature of the first order phase transition. A temporal extent of $N_\tau = 8$ provides $T/T_c = 0.91$ just below the critical temperature, T_c , and $N_\tau = 6$ provides $T/T_c = 1.22$ just above T_c .

3.1.2 Vortex density

Figure 2 provides an interactive rendering of the 3D structure of the centre vortex matter. To activate these illustrations and the animations to come, readers will need to open this document with Acrobat Reader or Foxit Reader. Click to activate, click and drag to rotate the image, control-click to translate and shift-click or mouse wheel to zoom into the image. The Views menu can be used to view specific features discussed in the text.

Even without activating the figures for closer inspection, one can see significant difference in the density of vortices. Above T_c the density drops from 1.8 to 1.2 fm^{-2} , approximately $2/3$ of the original density. Figure 10 of Ref. [1] illustrates the first order nature of the phase transition and the evolution of the vortex density with temperature.

3.1.3 Secondary clusters

The next clear signature of a phase transition is the suppression of secondary clusters in 3D temporal slices of the lattice. This is a robust deconfinement signature associated with the alignment of the vortex surface in four dimensions with the temporal axis.

In a study of $SU(4)$ gauge theory [33], animations of the vortex structure over temporal slices revealed how these secondary clusters migrate in the fourth dimension, thus providing a rendering of the two-dimensional vortex sheet in four dimensions. There one could see how the secondary clusters could migrate and eventually join the percolating structure.

A simplified illustration of this is provided in Fig. 3. The key requirement is that the vortex sheet curves back on itself in the temporal direction. The alignment of the vortex sheet with the temporal direction suppresses this curvature such that the number of secondary clusters drops significantly across the critical temperature. In essence, the absence of secondary clusters is a novel measure of vortex sheet alignment with the temporal direction. Figure 12 of Ref. [1] illustrates this significant drop across the phase transition, and the continued suppression of secondary clusters as one moves to higher densities.

3.1.4 Branching Points

Figure 15 of Ref. [1] shows a significant drop in the branching point density across the phase transition and this is also manifest in Fig. 2. In our visualisations illustrating the flow of centre

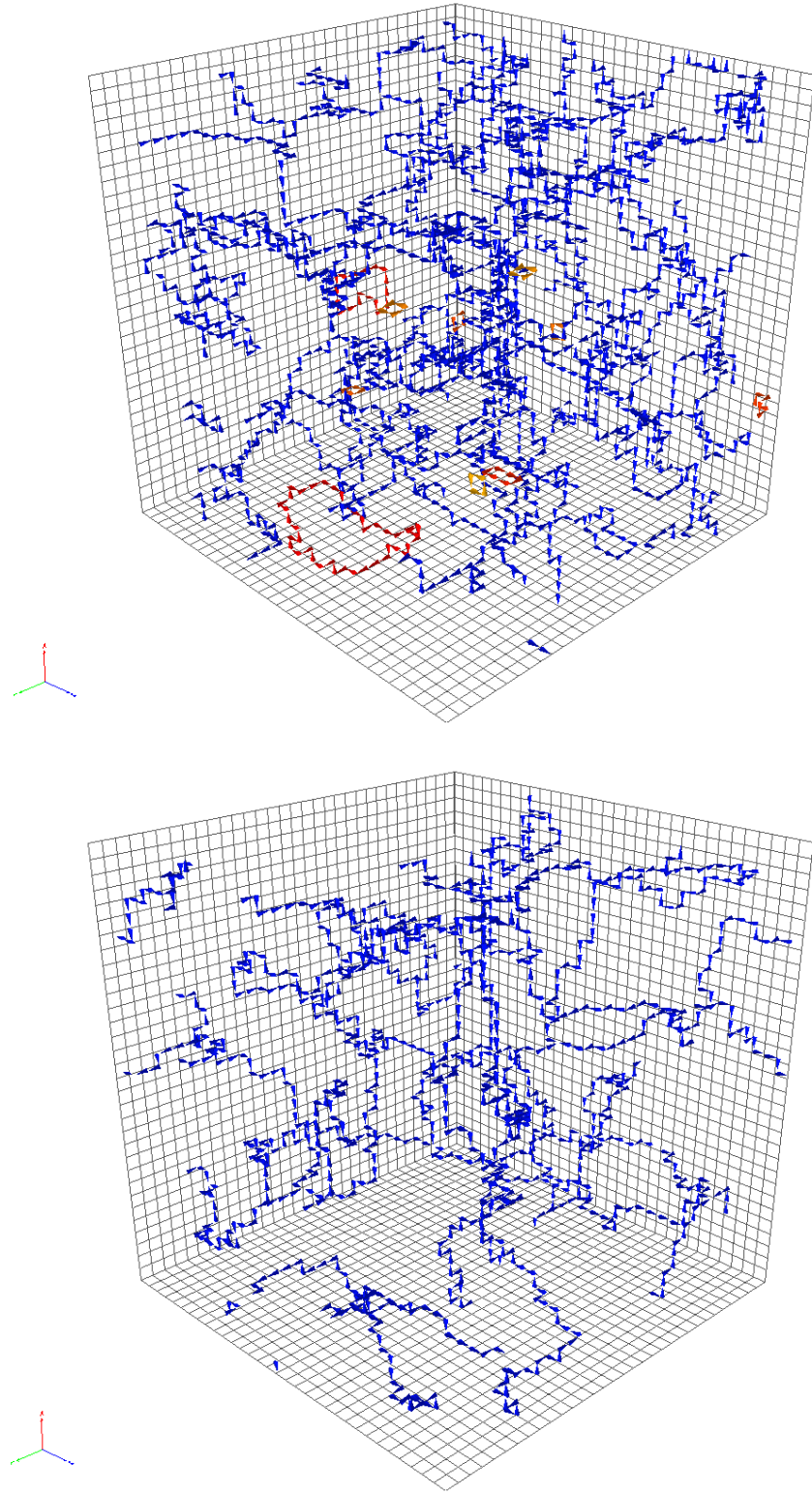


Figure 2: Illustrations of a temporal slice of the finite temperature lattices with $N_\tau = 8$ providing $T/T_c = 0.91$ (**upper**) and $N_\tau = 6$ providing $T/T_c = 1.22$ (**lower**). The blue jets illustrate the nontrivial plaquettes pierced by a vortex forming the percolating cluster. Secondary vortex clusters separate from the percolating cluster on this time slice are rendered in different colours to aid in their identification.

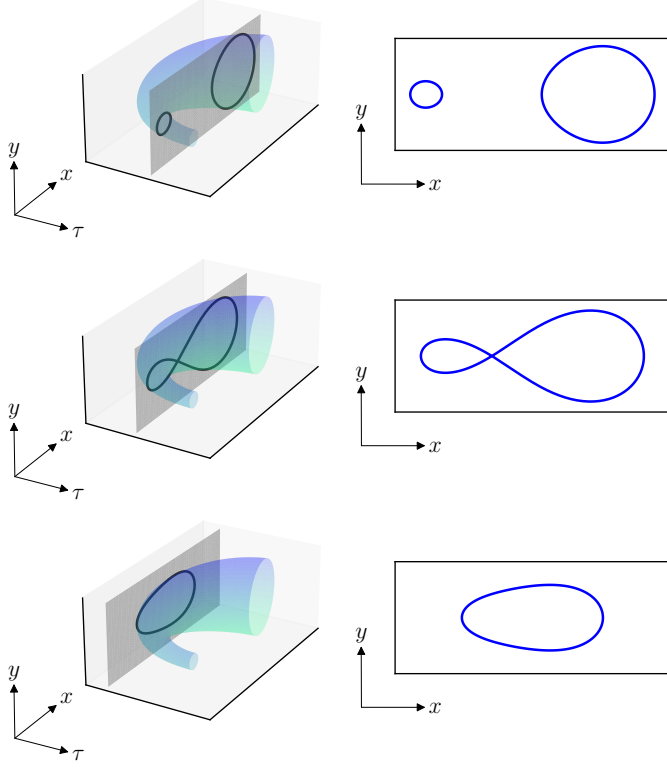


Figure 3: An simplified illustration showing how an apparently disconnected secondary cluster in a temporal slice of the lattice can be part of a single vortex sheet in four dimensions. Here, we are taking the equivalent of a temporal slice of the vortex surface by fixing the time coordinate (left column) and looking at an x - y cross section (right column). In the **top** illustration, the small loop in the fixed- τ cross section appears to disconnected from the larger loop. Because the surface curves back on itself in the temporal dimension, one can slice the surface at the time where the two loops connect (**middle**) to eventually form a single cluster (**bottom**). All loops belong to the same vortex sheet.

charge +1, these points appear as (anti-)monopoles with three jets converging or emerging from a cube of the lattice. Figure 4 reminds the reader of the relationship between monopoles and branching points.

While part of the reduction in branching point density can be attributed to a general loss of vortex density, the lower density is also manifest in the absence of vortex chains above T_c resembling knots. This feature is related to another characteristic of the first order phase transition, where there is a change in the tendency of branching points to cluster at low temperatures.

The suppression of branching-point clustering above T_c is illustrated in the histograms of vortex chain lengths between branching points in Fig. 17 of Ref. [1]. For temperatures below T_c there is a significant excess in small vortex chain lengths, well above the exponential fall off for larger chain lengths. This excess disappears across the phase transition as most clearly illustrated in the logarithmic vortex chain histograms in Fig. 19 of Ref. [1].

Returning to our temporal slice rendering in Fig. 2, an example of vortex clustering below T_c is provided in the “Branching point clustering” view in the upper rendering. There six branching

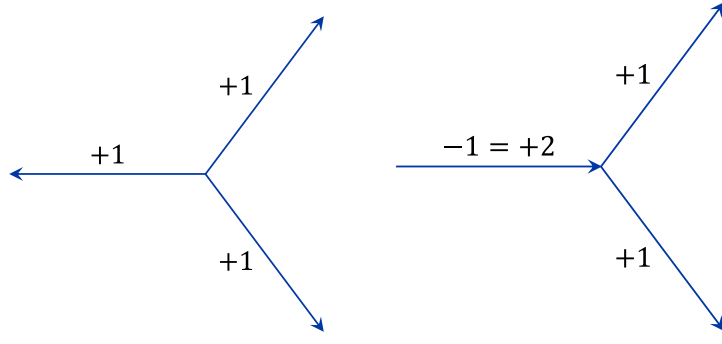


Figure 4: Schematic of a monopole vertex (**left**) versus a branching point (**right**). The monopole vertex follows our convention to illustrate the directed flow of $m = +1$ centre charge. Reversal of the left-hand arrow in the diagram shows the flow of charge $m = -1$, as seen on the right. Due to periodicity in the centre charge, $m = -1$ is equivalent to $m = +2$. Thus, the right-hand diagram depicts branching of centre charge.

points can been seen within the zoomed-in view. Three of these branching points are immediately adjacent to each other. Similar features do not appear above T_c . The view entitled ‘‘Linear vortex chains’’ shows an example of how the vortex chains tend to move away from a branching point in a linear manner without further branching in the immediate proximity.

Finally, it is worth noting that the branching point probability also drops across the phase transition as illustrated in Fig. 20 of Ref. [1]. This is a more subtle change that could not be confidently observed in the representative slices without the quantitative analysis of Ref. [1].

3.2 Spatial Slices

3.2.1 Overview

We now turn our attention to spatial slices of the lattice. Recall that it is these spatial slices that expose the space-time plaquettes relevant to the Wilson loop of Eq. (5) and confinement. Figure 5 provides representative visualisations of this vortex structure.

Four features are immediately apparent:

1. A large percolating cluster is absent above T_c signalling a loss of confinement. Below T_c a percolating vortex structure exists. Ample vortices pointing in the long spatial directions are available to pierce space-time Wilson loops and build an area law for confinement.
2. Secondary clusters remain present below T_c , despite the shorter temporal dimension. The view ‘‘Secondary cluster’’ in the upper rendering of Fig. 5 highlights the 10-jet vortex-chain loop that is separate from the percolating cluster in this slice.
3. Above T_c , the majority of vortices point in the temporal direction. As such, they are associated with spatial plaquettes and do not pierce a Wilson loop to create a confining potential. Thus, quark deconfinement is manifest above T_c .
4. The piercing of space-time plaquettes above T_c is rare, indicating an alignment of the vortex sheet in four dimensions with the temporal axis.

In the upper rendering of Fig. 5 there is a secondary cluster that wraps around the periodic time extent. The view ‘‘Periodic secondary cluster’’ highlights this structure. Below T_c , this vortex

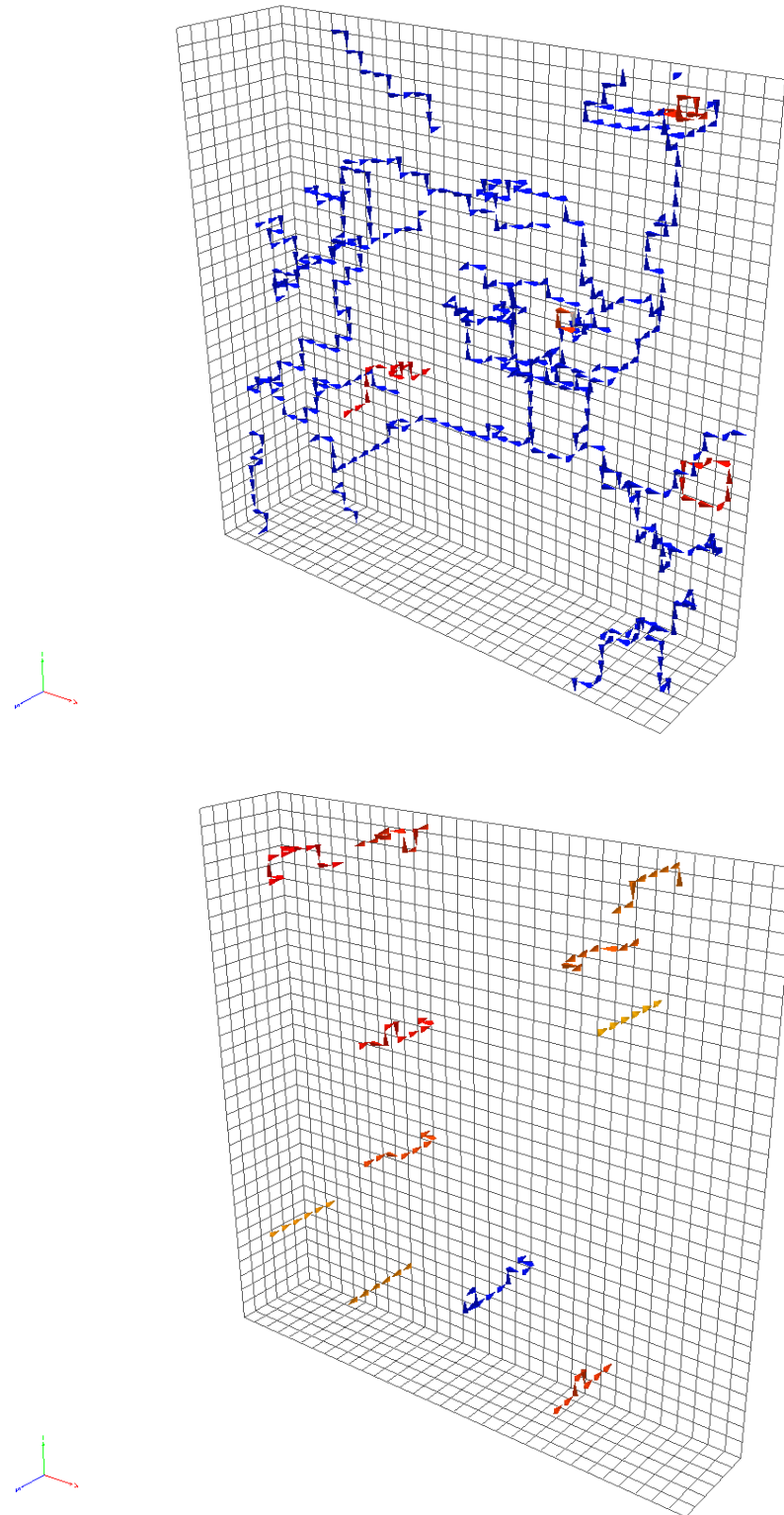


Figure 5: Illustrations of a spatial slice of the finite temperature lattices with $N_\tau = 8$ providing $T/T_c = 0.91$ (**upper**) and $N_\tau = 6$ providing $T/T_c = 1.22$ (**lower**). The blue jets illustrate the nontrivial plaquettes pierced by a vortex forming the percolating cluster. Secondary vortex clusters separate from the percolating cluster on this time slice are rendered in different colours to aid in their identification. Above T_c , most jets point in the short temporal direction, piercing spatial plaquettes and not generating confinement in space-time loops.

chain still pierces several space-time plaquettes, with 6 of the 14 jets potentially contributing to a Wilson loop. It is the straightening of this loop that signifies the deconfinement transition..

3.2.2 Vortex density

Turning our attention to the quantified properties of vortex matter, an even greater drop in the vortex density is observed in spatial slices as one crosses the critical temperature. Referring to Fig. 10 of Ref. [1], the robust first-order signal of the phase transition is the significant $\simeq 2/3$ drop in the vortex density from 1.9 to 0.6 fm^{-2} . This is manifest in Fig. 5.

3.2.3 Branching point density

Figure 15 of Ref. [1] shows a significant drop in the branching point density across the phase transition, from values approaching 2.9 fm^{-3} to 0.5 fm^{-3} across the phase transition, more than a five-fold reduction. This is also manifest in Fig. 2. A careful examination of the vortex chains in the lower rendering for $T/T_c = 1.22$ shows a single pair of branching points in the blue vortex chain. The view “Branching point pair” shows the two branching points with one split across the periodic boundary. Taking into account the 6×32^2 volume and the lattice spacing of 0.10 fm , this observation corresponds to a density of 0.3 fm^{-3} suggesting that one generally finds one to two pairs of branching points per slice.

4. Concluding Remarks

In this short presentation, we have revisited illustrations of vortex matter structure in pure SU(3) gauge theory in light of the quantitative analysis of Ref. [1] that demonstrates the first order nature of the deconfinement phase transition in the pure-gauge theory. Drawing on this analysis with references to the figures of Ref. [1], we have highlighted specific signatures of the established properties in the representative field structure illustrations. In a detailed side-by-side comparison of the vortex-matter field structure slightly below and above the critical temperature we have highlighted the vortex structure features that underpin the quantitative results. The abrupt step-change of the first order phase transition makes it easy to observe the field structure changes in the visualisations and animations.

Acknowledgements

It is a pleasure to acknowledge ongoing interesting discussions with Ryan Bignell and Chris Allton on the role of centre vortices in QCD ground state field structure and its associated gauge-invariant measures that quantify its properties. We also acknowledge the contributions of James Biddle in developing early vortex-geometry analysis techniques that continue to be of value. This work was supported with supercomputing resources provided by the Phoenix High Performance Computing (HPC) service at the University of Adelaide. This research was undertaken with the assistance of resources and services from the National Computational Infrastructure (NCI), which is supported by the Australian Government. This research was supported by the Australian Research Council through Grant No. DP210103706. W. K. was supported by the Pawsey Supercomputing Centre through the Pawsey Centre for Extreme Scale Readiness (PaCER) program.

References

- [1] J.A. Mickley, W. Kamleh and D.B. Leinweber, *Center vortex geometry at finite temperature*, *Phys. Rev. D* **110** (2024) 034516 [[2405.10670](#)].
- [2] J.A. Mickley, C. Allton, R. Bignell and D.B. Leinweber, *Center vortex evidence for a second finite-temperature QCD transition*, *Phys. Rev. D* **111** (2025) 034508 [[2411.19446](#)].
- [3] G. 't Hooft, *On the Phase Transition Towards Permanent Quark Confinement*, *Nucl. Phys. B* **138** (1978) 1.
- [4] G. 't Hooft, *A Property of Electric and Magnetic Flux in Nonabelian Gauge Theories*, *Nucl. Phys. B* **153** (1979) 141.
- [5] H.B. Nielsen and P. Olesen, *A Quantum Liquid Model for the QCD Vacuum: Gauge and Rotational Invariance of Domained and Quantized Homogeneous Color Fields*, *Nucl. Phys. B* **160** (1979) 380.
- [6] L. Del Debbio, M. Faber, J. Greensite and S. Olejnik, *Center dominance and Z(2) vortices in SU(2) lattice gauge theory*, *Phys. Rev. D* **55** (1997) 2298 [[hep-lat/9610005](#)].
- [7] M. Faber, J. Greensite and S. Olejnik, *Casimir scaling from center vortices: Towards an understanding of the adjoint string tension*, *Phys. Rev. D* **57** (1998) 2603 [[hep-lat/9710039](#)].
- [8] L. Del Debbio, M. Faber, J. Giedt, J. Greensite and S. Olejnik, *Detection of center vortices in the lattice Yang-Mills vacuum*, *Phys. Rev. D* **58** (1998) 094501 [[hep-lat/9801027](#)].
- [9] A. Montero, *Study of SU(3) vortex - like configurations with a new maximal center gauge fixing method*, *Phys. Lett. B* **467** (1999) 106 [[hep-lat/9906010](#)].
- [10] R. Bertle, M. Faber, J. Greensite and S. Olejnik, *The Structure of projected center vortices in lattice gauge theory*, *JHEP* **03** (1999) 019 [[hep-lat/9903023](#)].
- [11] M. Faber, J. Greensite, S. Olejnik and D. Yamada, *The Vortex finding property of maximal center (and other) gauges*, *JHEP* **12** (1999) 012 [[hep-lat/9910033](#)].
- [12] M. Engelhardt and H. Reinhardt, *Center projection vortices in continuum Yang-Mills theory*, *Nucl. Phys. B* **567** (2000) 249 [[hep-th/9907139](#)].
- [13] R. Bertle, M. Faber, J. Greensite and S. Olejnik, *P vortices, gauge copies, and lattice size*, *JHEP* **10** (2000) 007 [[hep-lat/0007043](#)].
- [14] M. Engelhardt, M. Quandt and H. Reinhardt, *Center vortex model for the infrared sector of SU(3) Yang-Mills theory: Confinement and deconfinement*, *Nucl. Phys. B* **685** (2004) 227 [[hep-lat/0311029](#)].
- [15] K. Langfeld, H. Reinhardt and J. Gattnar, *Gluon propagators and quark confinement*, *Nucl. Phys. B* **621** (2002) 131 [[hep-ph/0107141](#)].

- [16] J. Greensite, *The Confinement problem in lattice gauge theory*, *Prog. Part. Nucl. Phys.* **51** (2003) 1 [[hep-lat/0301023](#)].
- [17] K. Langfeld, *Vortex structures in pure SU(3) lattice gauge theory*, *Phys. Rev. D* **69** (2004) 014503 [[hep-lat/0307030](#)].
- [18] A. O'Cais, W. Kamleh, K. Langfeld, B. Lasscock, D. Leinweber, P. Moran et al., *Preconditioning Maximal Center Gauge with Stout Link Smearing in SU(3)*, *Phys. Rev. D* **82** (2010) 114512 [[0807.0264](#)].
- [19] P.O. Bowman, K. Langfeld, D.B. Leinweber, A. Sternbeck, L. von Smekal and A.G. Williams, *Role of center vortices in chiral symmetry breaking in SU(3) gauge theory*, *Phys. Rev. D* **84** (2011) 034501 [[1010.4624](#)].
- [20] E.-A. O'Malley, W. Kamleh, D. Leinweber and P. Moran, *SU(3) centre vortices underpin confinement and dynamical chiral symmetry breaking*, *Phys. Rev. D* **86** (2012) 054503 [[1112.2490](#)].
- [21] A. Trewartha, W. Kamleh and D. Leinweber, *Evidence that centre vortices underpin dynamical chiral symmetry breaking in SU(3) gauge theory*, *Phys. Lett. B* **747** (2015) 373 [[1502.06753](#)].
- [22] A. Trewartha, W. Kamleh and D. Leinweber, *Connection between center vortices and instantons through gauge-field smoothing*, *Phys. Rev. D* **92** (2015) 074507 [[1509.05518](#)].
- [23] J. Greensite, *Confinement from Center Vortices: A review of old and new results*, *EPJ Web Conf.* **137** (2017) 01009 [[1610.06221](#)].
- [24] A. Trewartha, W. Kamleh and D. Leinweber, *Centre vortex removal restores chiral symmetry*, *J. Phys. G* **44** (2017) 125002 [[1708.06789](#)].
- [25] J.C. Biddle, W. Kamleh and D.B. Leinweber, *Gluon propagator on a center-vortex background*, *Phys. Rev. D* **98** (2018) 094504 [[1806.04305](#)].
- [26] J.C. Biddle, W. Kamleh and D.B. Leinweber, *Visualization of center vortex structure*, *Phys. Rev. D* **102** (2020) 034504 [[1912.09531](#)].
- [27] J.C. Biddle, W. Kamleh and D.B. Leinweber, *Emergent Structure in QCD*, *EPJ Web Conf.* **245** (2020) 06009 [[2009.12044](#)].
- [28] J.C. Biddle, W. Kamleh and D.B. Leinweber, *Impact of dynamical fermions on the center vortex gluon propagator*, *Phys. Rev. D* **106** (2022) 014506 [[2206.02320](#)].
- [29] J.C. Biddle, W. Kamleh and D.B. Leinweber, *Static quark potential from center vortices in the presence of dynamical fermions*, *Phys. Rev. D* **106** (2022) 054505 [[2206.00844](#)].
- [30] A. Virgili, W. Kamleh and D. Leinweber, *Smoothing algorithms for projected center-vortex gauge fields*, *Phys. Rev. D* **106** (2022) 014505 [[2203.09764](#)].

- [31] J.C. Biddle, W. Kamleh and D.B. Leinweber, *Center vortex structure in the presence of dynamical fermions*, *Phys. Rev. D* **107** (2023) 094507 [[2302.05897](#)].
- [32] W. Kamleh, D.B. Leinweber and A. Virgili, *Numerical indication that center vortices drive dynamical mass generation in QCD*, *Phys. Rev. D* **110** (2024) L051502 [[2305.18690](#)].
- [33] J.A. Mickley, D.B. Leinweber and L.E. Oxman, *Structure of center vortex matter in SU(4) Yang-Mills theory*, [2502.19656](#).
- [34] D. Leinweber, J. Biddle, W. Kamleh and A. Virgili, *Dynamical fermions, centre vortices, and emergent phenomena*, *EPJ Web Conf.* **274** (2022) 01002 [[2211.13421](#)].
- [35] F. Gross et al., *50 Years of Quantum Chromodynamics*, *Eur. Phys. J. C* **83** (2023) 1125 [[2212.11107](#)].
- [36] Y. Iwasaki, K. Kanaya, T. Kaneko and T. Yoshie, *Scaling in SU(3) pure gauge theory with a renormalization group improved action*, *Phys. Rev. D* **56** (1997) 151 [[hep-lat/9610023](#)].